
IMPROVING THE ACCURACY OF INTERFERENCE MICROSCOPE MEASUREMENTS BY APPLYING GENETIC ALGORITHM

EZZAT ORABY ¹⁾, M. AMER ²⁾, T.Z.A. ABOU-ELNASR ³⁾, M. M. ELOKR ⁴⁾

1) *National Institute of Standards-Egypt, Al Haram, Tersa st., (ez Vao day nghe bai nay di ban
http://nhatquanglan.xlphp.net/zatoraby@hotmail.com, Tel: 020/01289732377)*

P.O.B. :136, code:12211, Fax: (+020)/33889783

2) *National Institute of Standards-Egypt, Al Haram, Tersa st., (amer_nis@yahoo.com)*

3) *Al-Azhar University- Egypt (prof_abouelnasr@yahoo.com)*

4) *Al-Azhar University- Egypt (moh_elokr@yahoo.com)*

Abstract

The interference microscope measurements with white light scanning interferometry (WLSI) and phase stepping interferometry (PSI) have been improved by optimizing the experimental conditions such as vertical distance between the objective and the surface under test (z), the tilt angles of the incident light beam with the surface and incident light intensity (I). Finally an accurate surface parameters measurement is obtainable. A genetic algorithm code has been developed to determine the best values of experimental conditions instead of manual adjustment by the operator. The combined uncertainty has been successfully reduced from 3.01 nm to 0.84 nm for the WLSI roughness measurement. While it has been reduced from 0.18 nm to 0.08 nm for the PSI step height measurement.

Keywords: *surface roughness, interference microscope, WLSI, PSI, genetic algorithm*

1. Introduction

1.1. Measurement conditions of interference microscope

For any measurement system, the total uncertainty is divided to type A and type B, the repeatability is the major component of type A. To obtain reliable surface parameter measurements of good repeatability in the interference microscope system, many sources of error have to be taken into account [1, 2]. Some sources of large significance are related to the computerized translational stage of the interference microscopy like vertical distance between the objective and the surface under test (z) and the tilt angles of the incident light beam with the examined surface: horizontal -or roll angle- (r) and vertical -or pitch angle- (p). Also the incident light intensity (I) illuminating the surface is considered.

Efficiency of any enhancing technique used for minimizing repeatability and then the uncertainty of measurement is estimated by studying the significant uncertainty components before and after the enhancing process. First the enhancing contribution to the repeatability should be studied and then the contribution of the repeatability itself to the total uncertainty.

Type B study which includes another set of error sources that have also been studied such as environmental noise of the system, flatness of internal reference plane, lateral calibration of objectives and vertical calibration of depth setting standard type A1 and type A2 (ISO 5436-1). However, a reference sphere is used for lateral and vertical calibrations.

1.2. Surface Metrology and artificial intelligence (AI)

A large number of researches interested in using *AI* in surface metrology has been issued such as designing inference engine for correlating surface texture parameters with functional measures [3], *Genetic algorithm (GA)* was used in phase recovery from the interferogram with minimum phase ambiguities [4], also different clustering techniques such as k-means, ISODATA and neural networks were used to relate surface metrology data to a component's function and the manufacturing process that produced the sample [5].

In this study the four measurement parameters: z , I , r , p have been studied, for each parameter separately using WLSI and PSI with an output expression of the *fitness* function used as a criterion for *image quality* (or *image completeness*) of the obtained image of the interference microscope. Precisely, fitness is the intensity of reflected light from the tested surface to the (Charge-Coupled Devices camera) CCD camera in the interference microscope system.

For each measurement of interference microscope system, the initial values of the four parameters are arranged as a four components vector (z, I, r, p) corresponding to a measurement fitness value. This vector is termed as a *solution* according to the GA terminology.

Once obtaining the optimum solution, the uncertainty components of type A and B are studied with this solution and then they are studied again but with manual adjusting (just using Metropro software directly with a moderately experienced operator).

2. Genetic algorithm code

The genetic algorithm is an evolutionary algorithm that belongs to the artificial intelligence techniques. It is a simulation of the natural selection and evolution in the biological science. A genetic algorithm code is developed to find an optimum measurement solution. Many of solutions are tested (*candidate solutions*) by calculating the corresponding *fitness* function for each one.

By running the measurements m times, a number of m solutions each with its fitness are stored to build up the initial population -*genome or generation*-. The solutions of the highest fitness values will possess the maximum probability to be *selected* as *successful fathers* to continue the evolution process in the next generation in the evolutionary cycle, that is so called *tournament selection*. Then the whole solutions of the first genome are applied to GA operators: *mating* -or exchange of some of components' values between successful fathers- and *mutation*

by inserting some values in random positions of the individual solutions. These operations are applied to the successive generations to ensure the convergence of the evolution process [6, 7]. The total evolution operation is explained in block diagram in Figure (1).

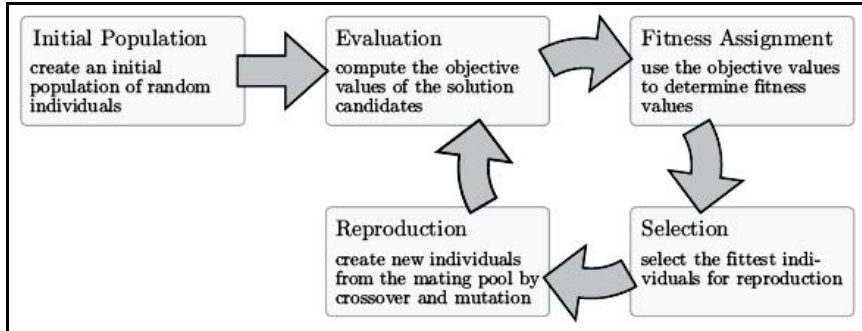


Fig.(1) The basic cycle of evolutionary algorithms

2.1. Assignment of fitness expression:

According to the most significant measuring parameters for white light scanning interferometry and phase stepping interferometry the fitness function has been chosen as follows:

2.1.1. Fitness for WLSI:

The direct number of points reflected from the surface to the CCD is considered as the fitness here, the largest number of points reflected, indicates an optimum reflection as the whole field of view of the sample is exposed to light normally [2] by adjusting angles (r) and (p), at the same time the incident light intensity has to be high enough to “see” all of surface details. On the other hand, care must be taken not to reach the CCD saturation conditions. In the two extreme cases some of reflected rays are lost, which leads to inaccurate parameters measurement.

2.1.2. Fitness for PSI:

PSI technique with monochromatic light is used in the applications such as step height measurement that need more precision than in scanning mode. The step height application is shown in Figure (2), where the sample area of interest is divided into three masked areas by the application software, the two areas on sides (reference) and the central flat step (test). The step height value is the net difference between reference and test masked areas. Unlike in roughness measurement in WLSI, the real number of the reflected points to the CCD cannot be taken into account in fitness expression, Instead, the PSI measurement is based on the root mean square plane of both reference and test masked areas, while the plane itself is

obtained from points reflected to the CCD, i.e. indirectly depends on the reflected points.

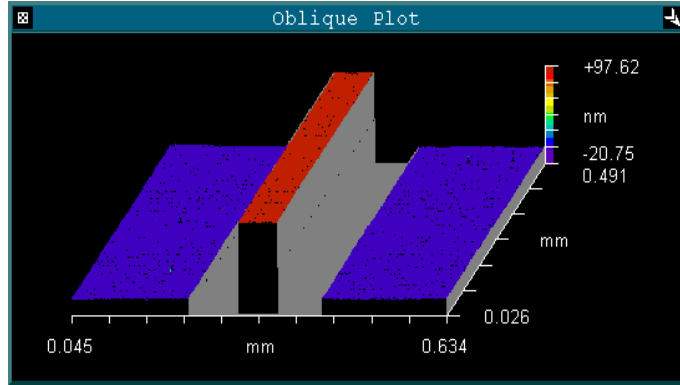


Fig. (2) 3d plot of step height by the interference microscope

An expression suggested by the author for fitness that based the fringe contrast of reference area, and inverse proportion with the tilt angles r and p . Many attempts finally lead to the following expression:

$$Fitness = \ln[FC/(30/T_x)(30/T_y)] \quad (1)$$

where: FC is the fringe contrast of reference area [8]

T_x and T_y are the tilt angles of the sample relative to the reference surface in x -direction and y -direction respectively [8]. The step height value is affected significantly with sample tilting T_x and T_y that are corresponding to the tilt angles r and p added to the parallelism error of the sample itself. The natural logarithm function (\ln) was helpful to minimize statistical dispersion of the data that will result as divergence of solutions.

3. Experimental procedures

Two specimens were tested, a roughness standard sample (Rubert) of nominal average roughness value (R_a) = 1000 nm used for WLSI mode with vertical range of 20 μm and a step height standard sample of nominal step height value (h) = 91.2 nm in the PSI mode where an optical filter is used to produce monochromatic light of λ = 633.4 nm with intensity averaging five times each run.

The used interferometer system is a Zygo interference microscope system New View Maxim GP 200 with 10X Mirau objective with the capability of WLSI and PSI. Once the optimum solution is reached i.e. the best conditions are obtained, the measurement is repeated with the optimum solution again more than five times to obtain the repeatability for the measured values in either WLSI or PSI mode.

3.1. Study of the significant components of uncertainty

3.1.1. Noise:

A silicon carbide optical flat (PTB certified) of waviness of 1 Angstrom is measured. The flat is measured twice at the same position while any averaging option is disabled to suppress any software de-noising option. The time duration between successive measurements or *runs* was as short as possible. Once the first evaluated topography had been obtained, it would have been considered to be a reference topography used as subtraction error topography for the next run programmatically by a written Metroscript code. As this pair of runs is repeated 20 times, the results will represent the residual vibration of the system.

3.1.2. Flatness of internal reference plane:

The above-mentioned flat is measured at sequential positions about 30 microns apart for each run, the larger the times of runs the closer flatness value from the reference plane flatness.

3.1.3. Lateral calibration of objectives

3.1.3.1. Linear grating:

A linear grating (VLSI Standard Inc.) of different scales was used to calibrate the lateral magnification for each objective by using the appropriate set of grating scales 10, 20, 50, 100 μm .

3.1.3.2. Reference sphere:

A sphere with a calibrated diameter ($R= 25.3998 \text{ mm}$) can alternatively be used to calibrate the objective axes X and Y together in one topography measurement. The Y-axis scaling is adjusted so that the residual flatness deviations reach a minimum level.

3.1.4. Depth setting standard type A1 (described in standard ISO 5436-1)

The depth setting standard A1 with calibrated groove *rectangular* shape is used to calibrate the scaling of the vertical axis of the microscope using PSI. A standard of certified step height values ($h= 44 \text{ nm}$) made by VLSI Standard Inc. was used. Another A1 standard was also used to confirm the linearity of the vertical performance with *largely* different length from the first, It is made by Taylor Hobson and certified by KRISS-Korean ($h=2.281 \mu\text{m}$), it was measured by WLSI of proven reliability for heights measuring as will be described in the next section [9, 10].

3.1.5. Depth setting standard type A2 (described in standard ISO 5436-1)

A depth setting standard with four calibrated grooves of *rounded* bottom traceable to PTB is used to verify the calibration at several depths to give a control for the linearity of the system. The depth is derived from the deepest point of the

parabola which fits the bottom of the groove. The used WLSI does not have 2π ambiguity compared to optical phase shift interferometry [9, 10, 11].

4. Results and discussion

4.1. Scanning mode:

As shown in figure (3a) by running the genetic code with fitness standard deviation limit = 3000 and mutation probability = 0.2 the fitness convergence has been detected at run 80 (eighth genome) leading to an optimum value of Ra = 946 nm as shown in Ra convergence in Figure (3b)

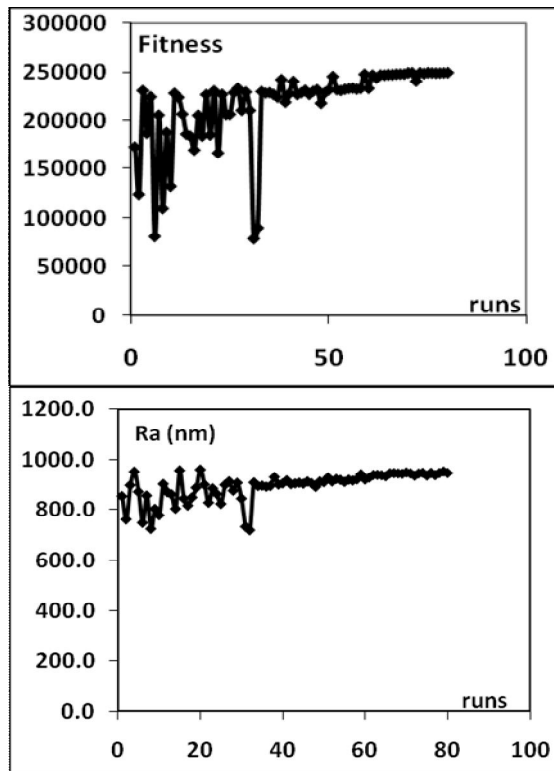


Fig.(3a) and (3b) Fitness convergence and the corresponding Ra convergence in scanning mode

4.1.1. Repeatability:

By manual adjusting of the measurement parameters, an average roughness value of 942.7 nm of repeatability 8.5 nm was obtained, while by using the genetic code the step height average = 946.2 nm with repeatability = 2.3 nm as shown in Figure (4)

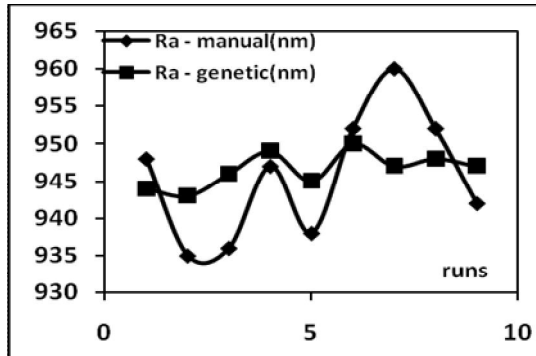


Fig.(4) Repeatability of Ra using Metropro using both genetic code and Metropro direct

4.2. Phase stepping mode:

As shown in Figure (5a) and (5b) by running the genetic code with fitness standard deviation limit = 0.1 and mutation probability = 0.1, the fitness convergence has been detected at run 71 (seventh genome) leading to an optimum value of step height (h) = 90 nm as shown in height convergence in Figure (5b). The value obtained by genetic code was found to be in agreement with the value measured by WLSI technique for which reliable results are obtained but of less repeatability than PSI.

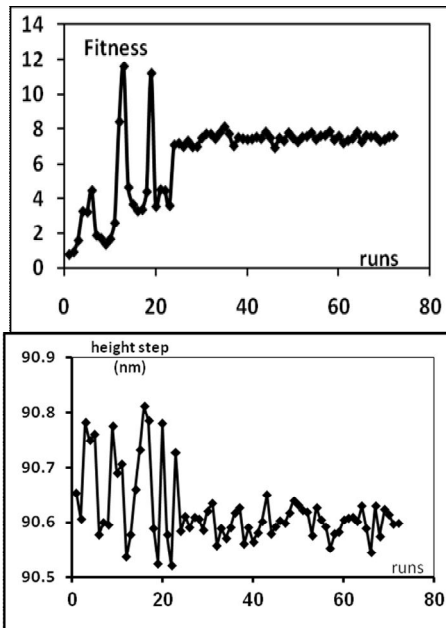


Fig.(5a) and (5b) Fitness convergence and step height convergence in phase stepping mode

4.2.1. Repeatability

By manual adjusting of the measurement parameters (just using Metropro software directly as mentioned above) a step height average value of 90.7 nm of repeatability 0.4 nm , while by using the genetic code the step height average = 90.6 nm with repeatability = 0.05 nm as shown in Figure (6).

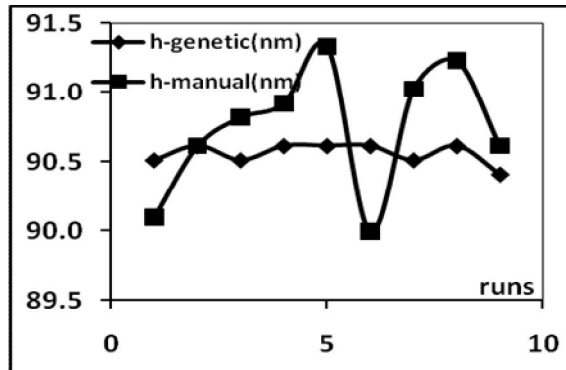


Fig.(6) Repeatability of step height using both genetic code and Metropro direct Calibration of interference microscope

4.3. Results for Significant components of uncertainty

The results are outlined in form of values and graphs and finally the uncertainty budget of the studied components for WLSI and PSI are shown below:

The system noise = 0.2 nm with standard deviation ($\sigma = 0.08$ nm)

Flatness of internal reference plane = 0.23 nm with standard deviation ($\sigma = 0.1$ nm) Lateral calibration of objective

4.3.1. Linear grating:

Figure (7) shows the results for lateral calibrations of all objectives the symbol 5X-X stands for the X-axis of the objective 5X and so on. Each objective is calibrated with a pair of appropriate scales indicated on graphs to confirm the linearity of lateral performance.

4.3.2. Reference sphere:

The results of o calibration - in X and Y directions - using standard sphere is outlined in Figure (8) as a comparison between the certified value and values using all objectives at the Egyptian National Institute for Standards (NIS).

4.3.3. Depth setting standard type A1 (ISO 5436-1)

Figures (9) and (10) show the measurement of setting standards A1 type using PSI and WLSI techniques respectively

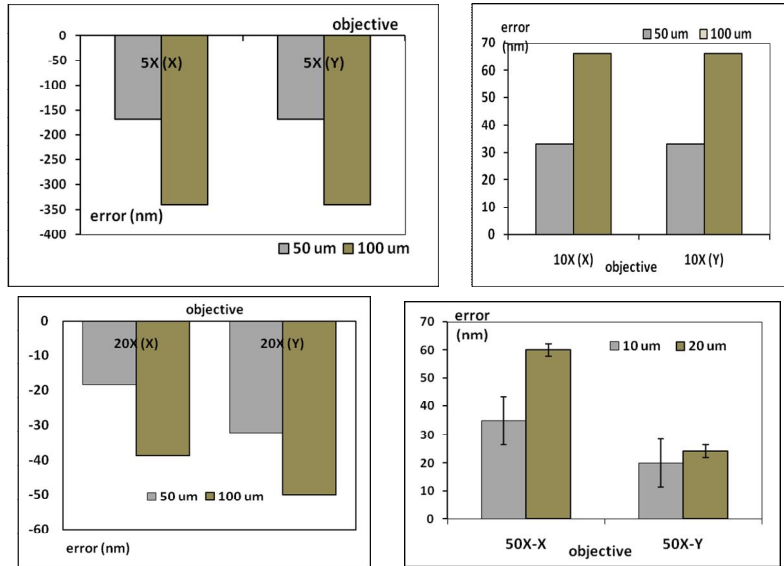


Fig.(7) Error or deviation of objectives 5X, 10X, 20X, 50X readings from nominal values of grating scales

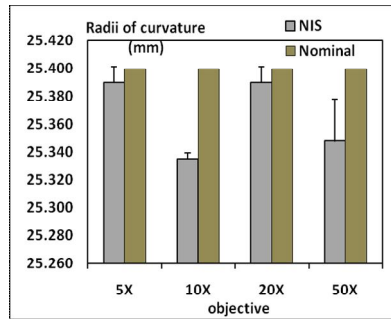


Fig.(8) Radii of curvature of the standard sphere measured by the four objectives 10X-50X at the and compared to the nominal value

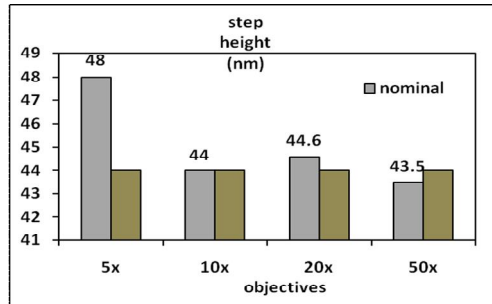


Fig.(9) Calibration results of the step height of type A1 of nominal value h = 44 nm using PSI with $\lambda = 633.4$ nm

The step height standard A1 of certified value of $h = 2.281 \mu\text{m}$ with combined uncertainty of $0.0038 \mu\text{m}$ (KRISS), while it was measured at NIS as $2.286 \mu\text{m}$ with repeatability of $0.002 \mu\text{m}$

4.3.4. Depth setting standard type A2 (ISO 5436-1)

Figures (10-a, b) show the measurement of setting standards A2 type using WLSI technique

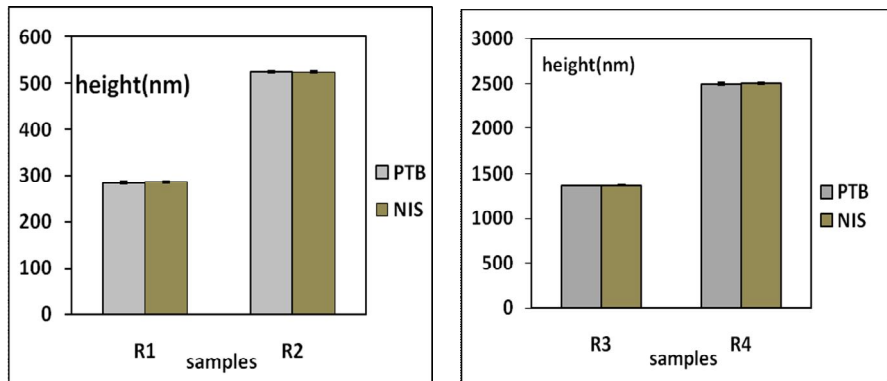


Fig.(10 a, b) Calibration results of the step height of type A2 by PTB of certified values (a) $h = 284 \text{ nm}$, 524 nm (b) $h = 1365 \text{ nm}$, 2498 nm using WLSI, all compared with results at (NIS)

4.4. Uncertainty budget according to the studied components

4.4.1. for roughness measurement using objective Mirau type 10X

Table (1) Uncertainty budget of some significant components of the roughness measurement

source	standard uncertainty u_i	Degree of freedom n	sensitivity c_i	Combined unc. component $u_{ic} = u_i * c_i / \sqrt{(n-1)}$
noise nm	0.200	20	1	0.046
ref flatness nm	0.23	16	1	0.059
L grating %	0.624	5	0	0.000
radius of curvature %	0.568	10	1	0.189
depth setting standard A1	0.660	5	1	0.330
depth setting standard A2	0.946	3	1	0.669
repeatability nm	8.500	9	1	3.005
U_c	3.03 nm			
$U_{95\%} = k * U_c$	6.06 nm			

According to Table 1, the relative contribution of the repeatability component to the total uncertainty is: $u_{rep}/U_c = 3.005/3.03 = 99\%$. By applying the genetic optimization the repeatability is reduced to $u_{rep} = 0.813 \text{ nm}$, by substitution this

value into Table 2 , the combined uncertainty becomes: $U_c = 0.9$ nm instead of 3.03 nm

4.4.2. for step height measurement using objective Mirau type 10X

Table (2) uncertainty budget of some significant components of the step height measurement

Source	standard uncertainty u_i	Degree of freedom n	sensitivity c_i	Combined unc. component $u_{ic} = u_i * c_i / \sqrt{(n-1)}$
<i>noise nm</i>	0.200	20	1	0.046
<i>ref flatness nm</i>	0.230	16	1	0.059
<i>L grating %</i>	0.060	5	0	0.000
<i>radius of curvature %</i>	0.055	10	1	0.018
<i>depth setting standard A1 nm</i>	0.064	5	1	0.032
<i>depth setting standard A2 nm</i>	0.912	3	1	0.645
<i>repeatability nm</i>	0.450	9	1	0.159
U_c	0.18 nm			
$U_{95\%} = k*U_c$	0.36 nm			

Applying the same calculations to Table 2, the relative contribution of the repeatability to the total uncertainty is: $u_{rep}/U_c = 0.159/0.180 = 89\%$. By applying the genetic optimization the repeatability is reduced to $u_{rep} = 0.05$ nm, by substitution this value into Table 2 the combined uncertainty becomes $U_c = 0.09$ nm instead of 0.18 nm

References

1. Zehra Sarac, Reinhard Gro, Claus Richter, Bernhard Wiesner, "Optimization of white light interferometry on rough surfaces based on error analysis", Gerd Hausler Optik, 115, No. 8 (351–357), <http://www.elsevier.de/ijleo>, 2004.
2. Richard Leach ,Leigh Brown, Xiangqian Jiang, "Measurement Good Practice Guide No. 108 Guide to the Measurement of Smooth Surface Topography using Coherence Scanning Interferometry", NPL, (30-36), 2008.
3. [3] B. Muralikrishnan, J. Raja, "Inference engine for process diagnostics and functional correlation in surface metrology", Wear 257 (1257–1263), 2004.
4. S.K. Ghorai, Dilip Kumar, Baljeet K Hura, "Strain measurement in a Mach–Zehnder fiber interferometer using genetic algorithm" Sensors and Actuators A 122 (215–221), 2005.
5. B. Muralikrishnan, K. Najarian, J. Raja, "Process Mapping and Functional Correlation in Surface Metrology: A novel clustering application", The International Journal of Advanced Manufacturing Technology, November, Volume 27, Issue 1-2 (75-82), 2005.
6. Thomas Weise, "Global Optimization Algorithms Theory and Application" <http://www.it-weise.de/>, (72, 105, 120), 2008.

7. Randy L. Haupt, "Practical Genetic Algorithm"; wiley interscience, (85-90), 2004
8. MetroPro Reference Guide OMP-0347H, Zygo corporation, www.zygo.com, (9-10), 1999
9. R. Kruger-Sehm , J.A. Luna Perez, "Proposal for a guideline to calibrate interference microscopes for use in roughness measurements", International Journal of Machine Tools & Manufacture, 41 (2123–2137), 2001
10. ISO 5436-1, "Geometrical Product Specifications GPS Surface texture: Profile method; Measurement standards – Part1 Material measures", (1-5), 2001
11. Taehyun Kim, MooJong Kim, Ho-Sang Kim, Chan-Hee Lee and Moon G. Lee, "Measurement and Analysis of Micro Lens Array using White Light Scanning Interferometer", The 10th international symposium of measurement technology and intelligent instruments, (1-2), 2011